Science Advances
AAAS

Supplementary Materials for

North Atlantic cooling triggered a zonal mode over the Indian Ocean during Heinrich Stadial 1

Xiaojing Du *et al.*

Corresponding author: Xiaojing Du, xiaojing_du@brown.edu

Sci. Adv. **9**, eadd4909 (2023)
DOI: 10.1126/sciadv.add4909

This PDF file includes:

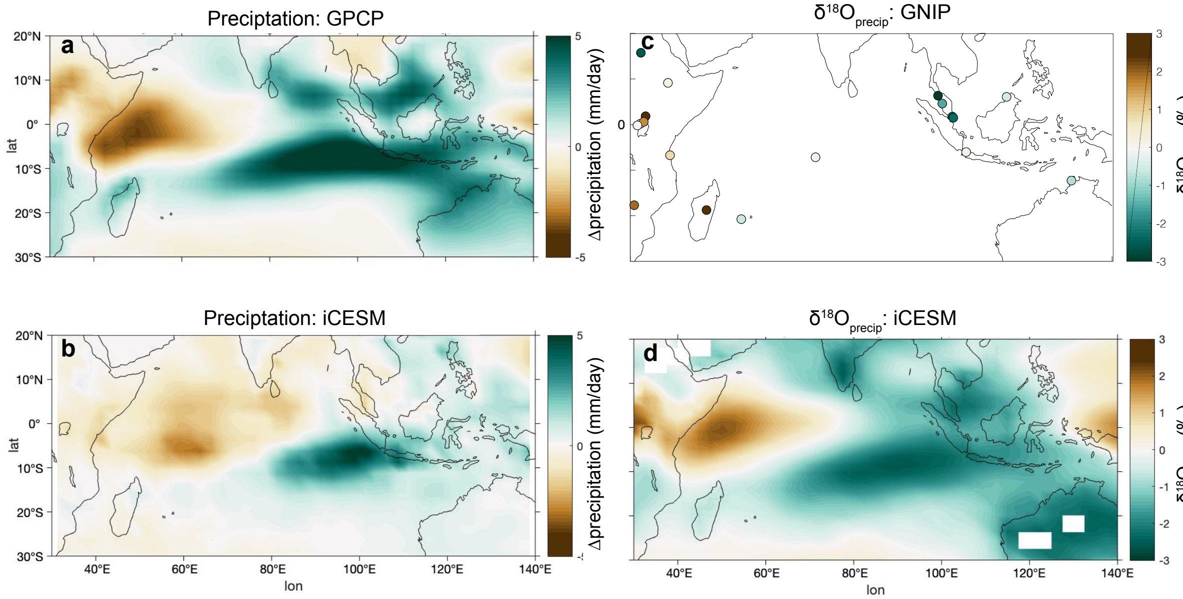

Fig. S1 Precipitation and $\delta^{18}O_{precip}$ anomalies of negative IOD events minus positive IOD events in modern observations and iCESM. (a) Observed precipitation anomalies from the Global Precipitation Climatology Program (GPCP) from 1979-2020 (*58*). (b) Precipitation anomalies for iCESM from 1850-2005. (c) $\delta^{18}O_{precip}$ anomalies for GNIP observations spanning 1961-2016. (d) $\delta^{18}O_{precip}$ anomalies for iCESM from 1850-2005. Negative and positive IOD events are defined as intervals when the IOD Index (https://psl.noaa.gov/gcos_wgsp/Timeseries/DMI/) exceeds and falls below 0.4°C, respectively. IOD index is defined as the anomalous surface temperature gradient between western equatorial Indian Ocean (50˚E-70˚E and 10˚S-10˚N) and the southeastern equatorial Indian Ocean (90˚E-110˚E and 10˚S-10˚N)

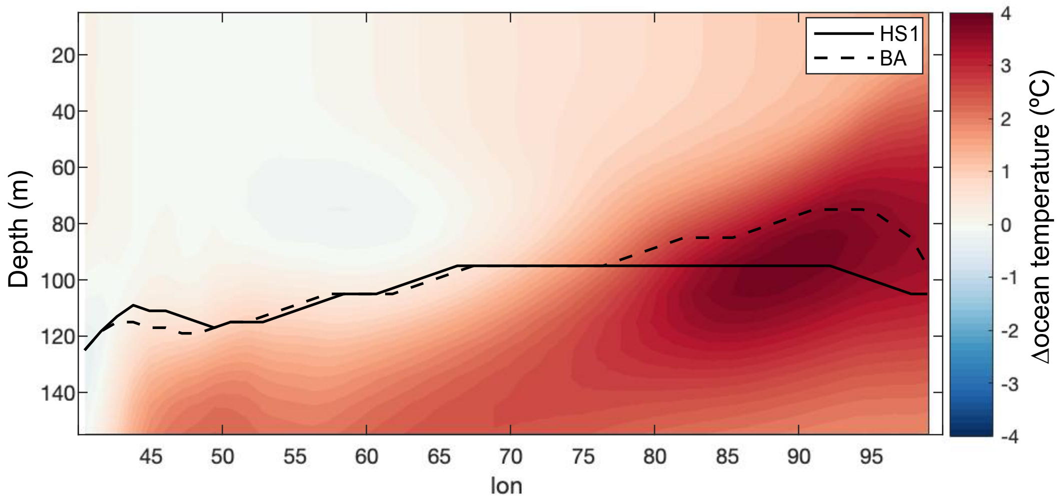

Fig. S2 Simulated changes in subsurface ocean temperature (shading) over the equatorial Indian Ocean (40˚E–100˚E, 10˚N –10˚S) during HS1 relative to BA due to meltwater flux effect (MWF) in iTRACE. Solid and dashed black curve indicate the depth of thermocline during HS1 and BA, respectively, calculated as the depth of maximum vertical temperature gradient.

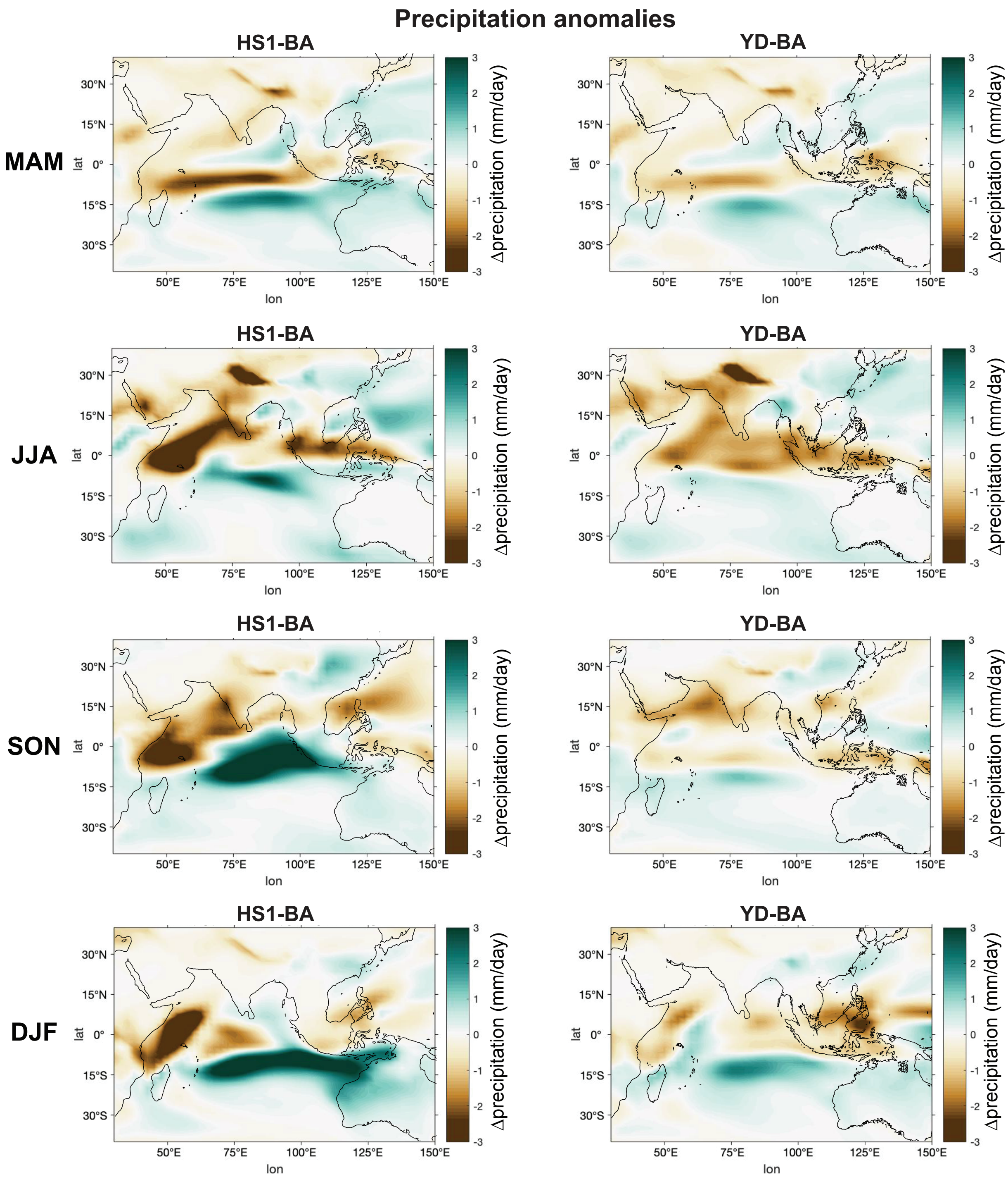

Fig. S3 Simulated changes in precipitation in response to meltwater flux effect (MWF) during HS1 and YD (relative to BA) in boreal spring (MAM), summer (JJA), fall (SON), and winter (DJF). Coastlines (black outline) for HS1 and YD correspond to 120 m and 60 m drop in sea level, respectively.

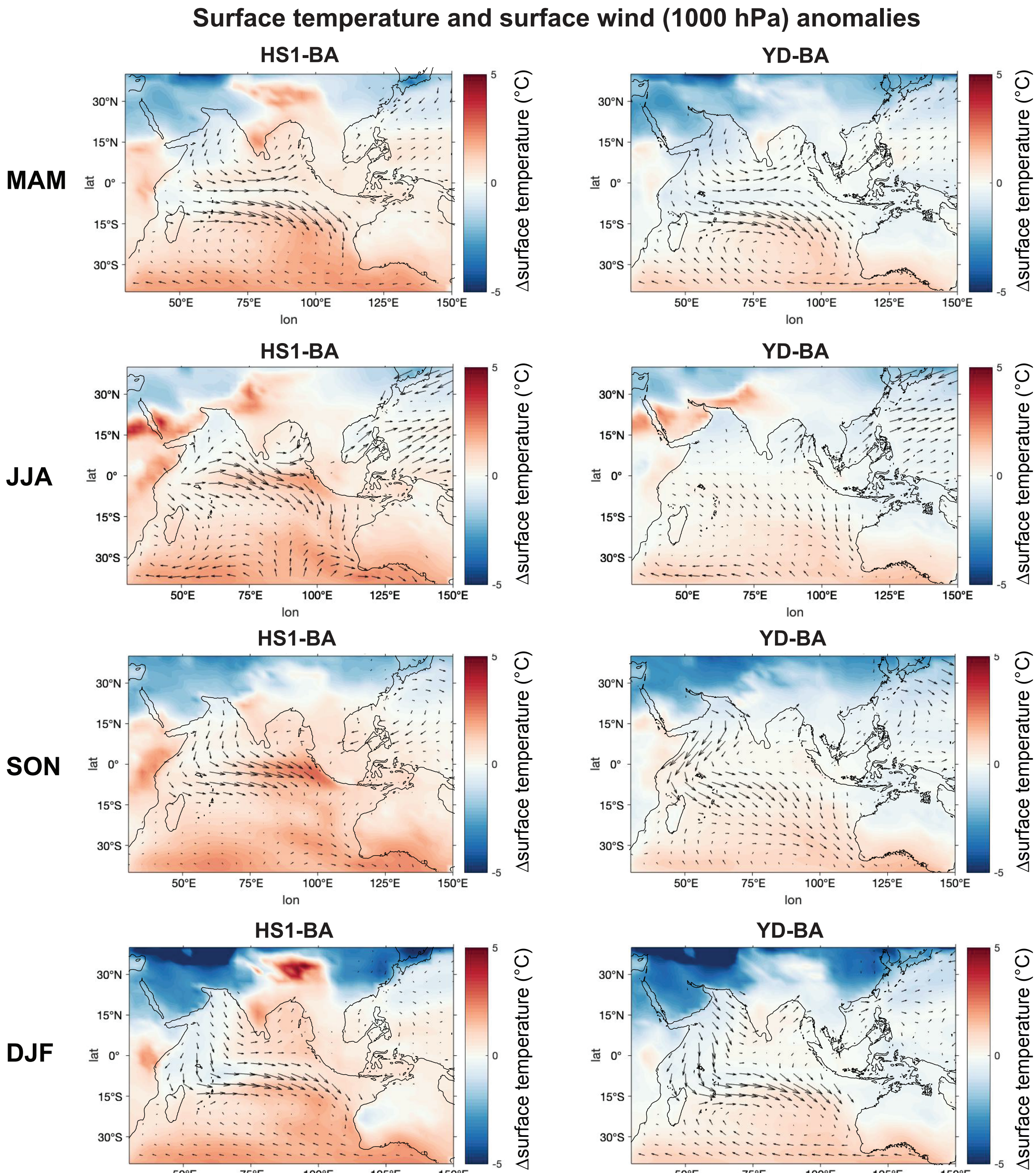

Fig. S4 Simulated changes in surface temperature and surface wind (1000 hPa) in response to meltwater flux effect (MWF) during HS1 and YD (relative to BA) in boreal spring (MAM), summer (JJA), fall (SON), and winter (DJF). Coastlines (black outline) for HS1 and YD correspond to 120 m and 60 m drop in sea level, respectively.

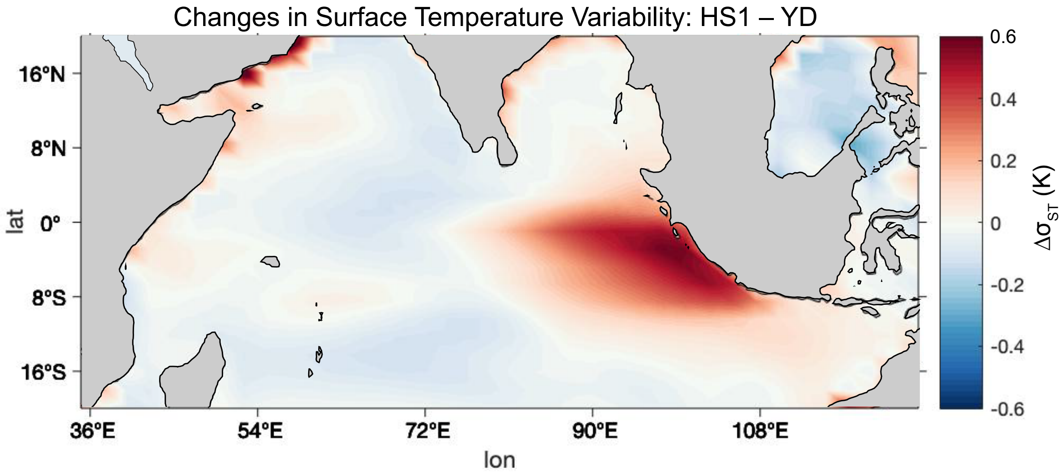

Fig. S5 Simulated changes in Indian Ocean interannual surface temperature variability between HS1 and YD due to ice sheets and paleogeography (ICE run) in iTRACE. The changes in surface temperature variability are computed as the difference in standard deviation of 2–10-year bandpass filtered, monthly-resolved surface temperature during HS1 and YD. This result suggests increased climate variability over IO in response to the exposure of Sunda and Sahul shelves under glacial boundary conditions, in consistent with previous proxy (*32*) and model simulation (*33*) studies. Black outline and gray shadow indicate HS1 coastlines corresponding to a 120 m drop in sea level.

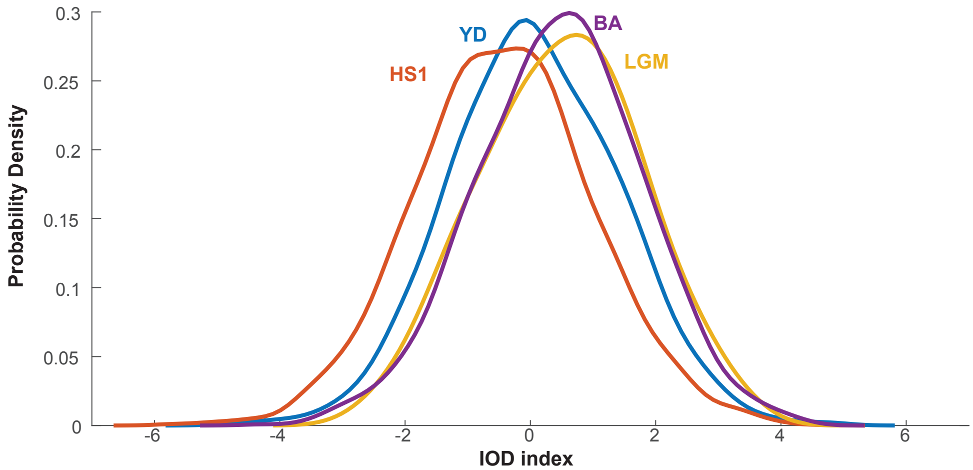

Fig. S6 Probability density functions (PDFs) of simulated fall (Sep-Nov) Indian Ocean Dipole (IOD) index in iTRACE in response to meltwater flux (MWF) effect, during LGM (19-20 ka, yellow), HS1 (14.5–18 ka, red), BA (14.5-12.9 ka, purple), and YD (11.7 –12.9 ka, blue). IOD index is defined as the anomalous surface temperature gradient between western equatorial Indian Ocean (50˚E-70˚E and 10˚S-10˚N) and the southeastern equatorial Indian Ocean (90˚E110˚E and 10˚S-10˚N). PDF estimates were computed using a kernel density estimation method (*64*).

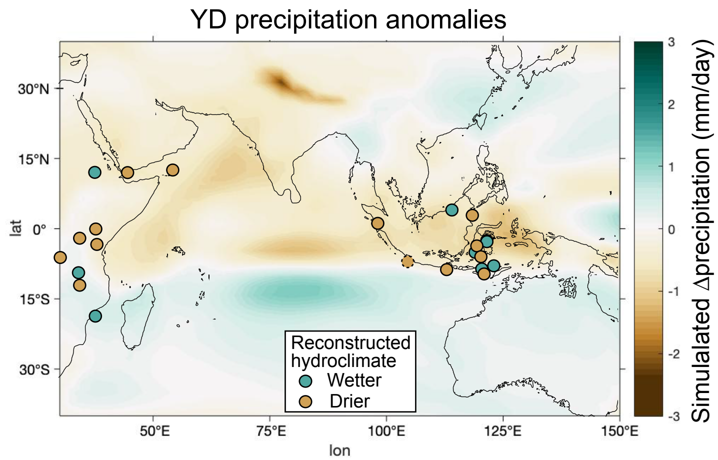

Fig. S7 Proxy-model synthesis of precipitation anomalies during YD relative to BA in response to meltwater flux in iTRACE. The network of precipitation-sensitive proxies includes speleothem $\delta^{18}O$, leaf wax δD, detrital flux, pollen, and lake level, capturing drier (brown) or wetter (green) conditions at YD. All speleothem $\delta^{18}O$ and leaf wax δD values have been corrected for global ice volume effects on the isotopic composition of sea water. Dashed circles represent sites where YD anomalies records are less robust due to chronologic uncertainties or low temporal resolution (see Methods for details). Black outline indicates YD coastlines corresponding to a 60 m drop in sea level.

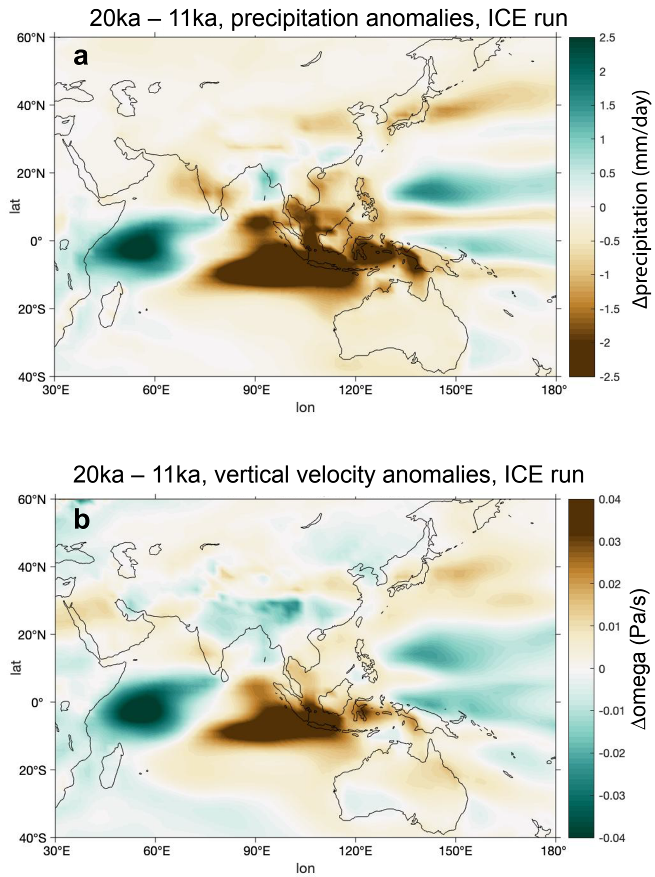

Fig. S8 Simulated changes in annual (a) precipitation and (b) vertical velocity (omega) at 500 hPa level from the Last Glacial Maximum to early Holocene (20ka minus 11ka) in response to ice sheets and paleogeography (ICE run) in iTRACE. The exposure of Sunda and Sahul shelves due to lower glacial sea level leads to weaker Walker circulation across the IO, indicated by reduced convection (anomalously positive omega) with drying conditions in eastern IO, and intensified convection (anomalously negative omega) with wetter conditions over the western IO.

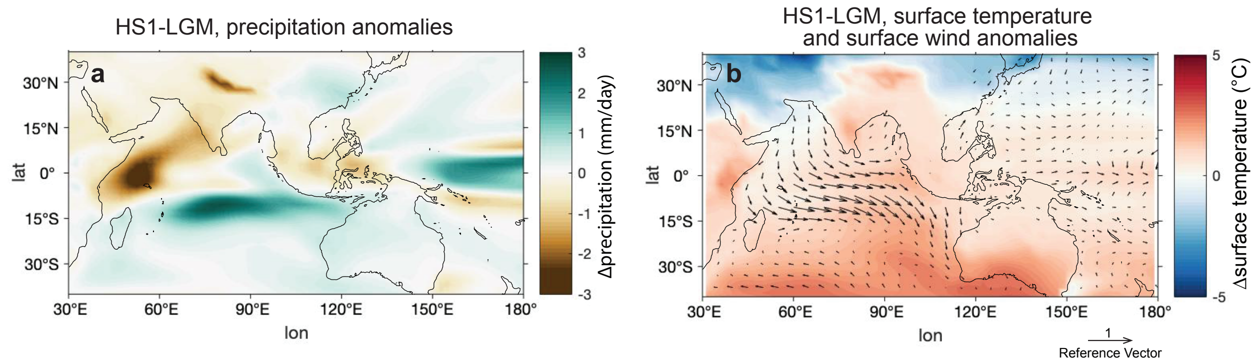

Fig. S9 Simulated changes in annual (a) precipitation and (b) surface temperature and surface wind (1000 hPa) from the Last Glacial Maximum to early Holocene (20ka minus 11ka) in response to meltwater flux effect (MWF) in iTRACE. Black outline indicates HS1 coastlines corresponding to a 120 m drop in sea level.

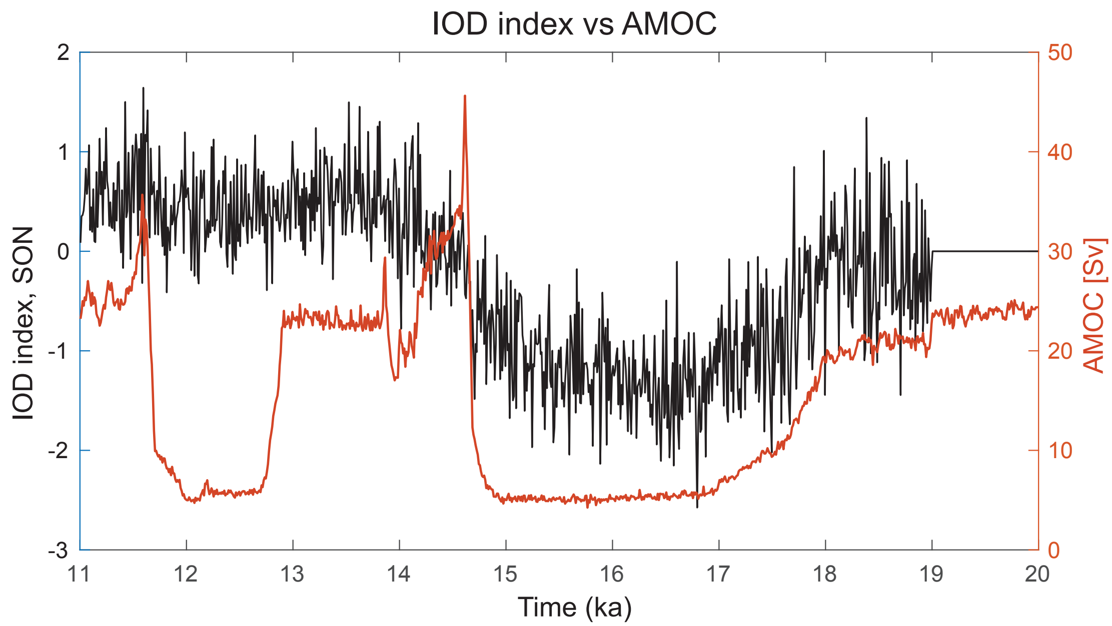

Fig. S10 Simulated changes in fall (Sep-Nov) Indian Ocean Dipole (IOD) index (black) in response to meltwater flux (MWF) effect, and AMOC intensity (red) in iTRACE.

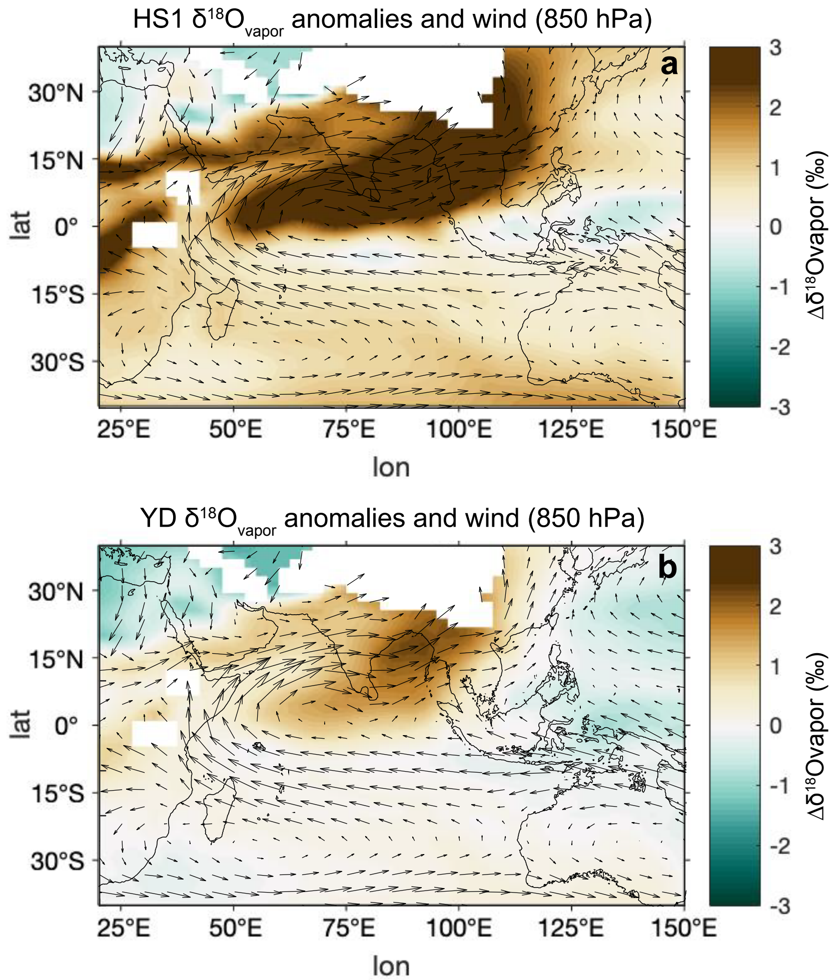

Fig. S11 Simulated summer (June to August) d$^{18}O_{vapor}$ anomalies during (a) Heinrich stadial 1 (HS1) and (b) Younger Dryas (YD) relative to Bølling-Allerød in response to meltwater flux in iTRACE. The wind field in (a) and (b) represent mean conditions during HS1 and YD, respectively. Coastlines (black outline) for HS1 and YD correspond to 120 m and 60 m drop in sea level, respectively.

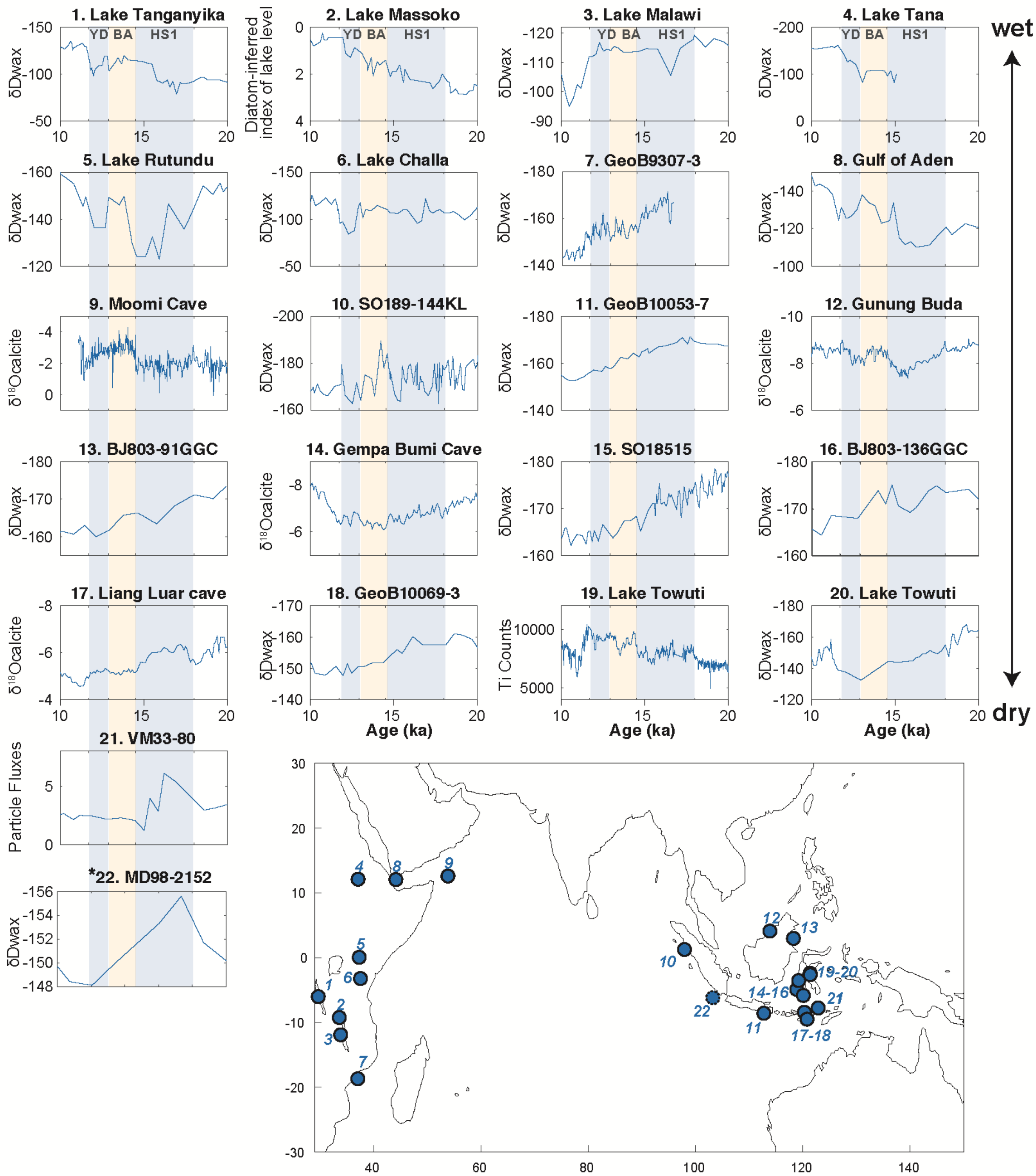

Fig. S12 Precipitation-sensitive records included in the proxy synthesis. The dDwax record from core MD98-2151 (marked with *) only contains one data point during BA. The interpretation of precipitation change from Lake Rukwa and Lake Victoria are inferred from pollen and lake level records following Vincens et al. (*62*) and Stager et al. (*63*), respectively, and are not shown here.

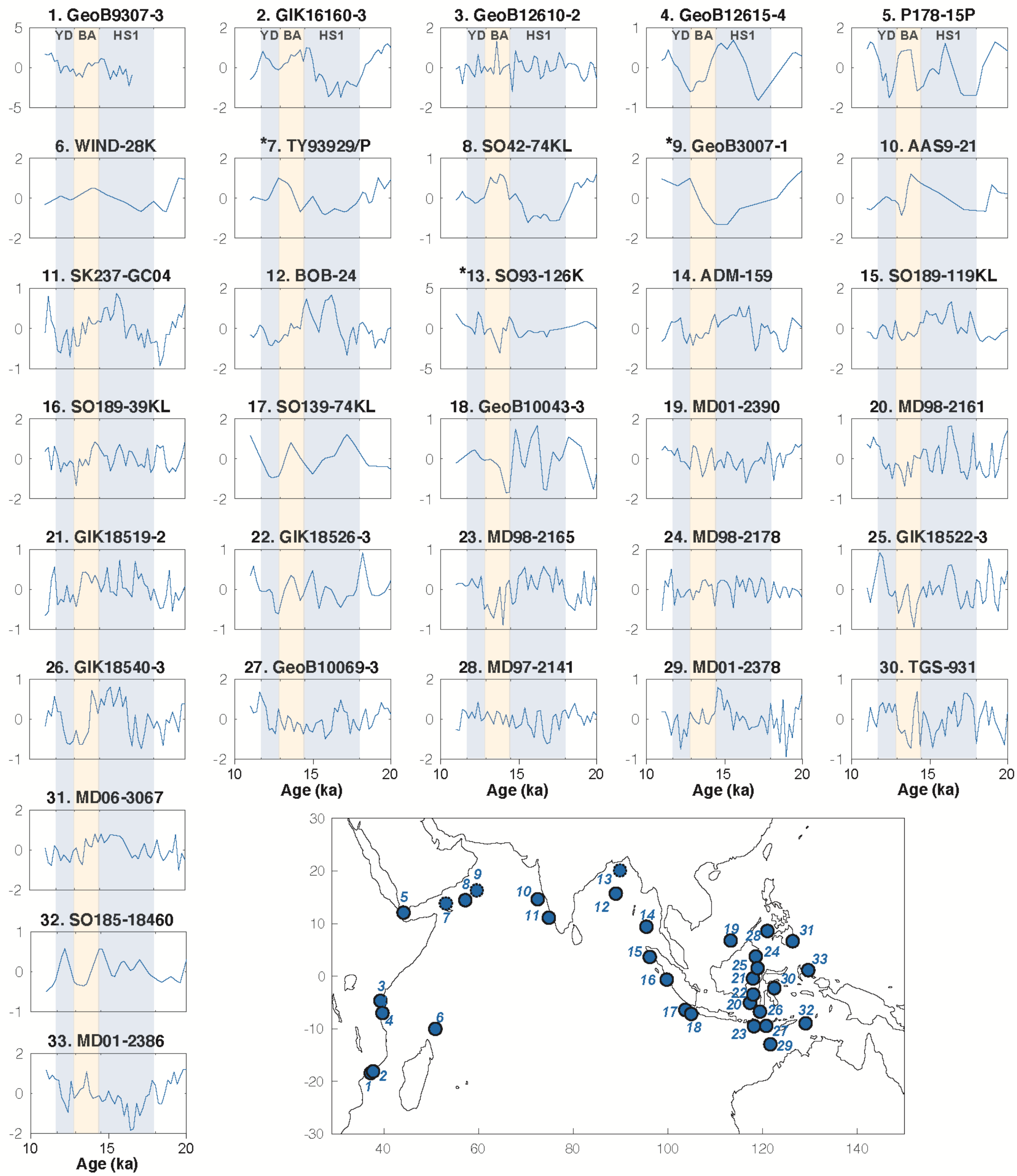

Fig. S13 SST records involved in the proxy synthesis in this study. Records whose chronology are based on oxygen isotope stratigraphy are marked with star (*).

Table S1. List of the precipitation-sensitive proxy data involved in the proxy synthesis in this study.

Region/Country	Site/Core ID	Lat	Lon	Proxy	Category	References
East Africa	Lake Tanganyika	-6.10	29.83	δDwax	Dry	Tierney et al. (*40*)
Tanzania	[a]Lake Rukwa	-8.00	32.00	pollen	Dry	Vincens et al. (*62*)
Tanzania	Lake Massoko	-9.33	33.75	lake level	Dry	Barker et al. (*65*)
Malawi	Lake Malawi	-12.00	34.00	δDwax	Dry	Konecky et al. (*39*)
Kenya/Uganda/Tanzania	[a]Lake Victoria	-2.00	34.00	lake level	Dry	Stager et al. (*63*)
Ethiopia	Lake Tana	12.00	37.25	δDwax	Dry	Costa et al. (*66*)
Mozambique channel	GeoB9307-3	-18.57	37.38	δDwax	Wet	Schefuß et al. (*13*)
Kenya	Lake Rutundu	-0.04	37.46	δDwax	Dry	Garelick et al. (*67*)
Kenya/Tanzania	Lake Challa	-3.32	37.70	δDwax	Dry	Tierney et al. (*68*)
Gulf of Aden	P178-15P	11.96	44.30	δDwax	Dry	Tierney and DeMenocal (*69*)
Yemen	Moomi Cave	12.50	54.00	$\delta^{18}O_{calcite}$	Dry	Shakun et al. (*70*)
off Sumatra	SO189-144KL	1.16	98.07	δDwax	Dry	Niedermeyer et al. (*22*)
off Sumatra	[b]MD98-2152	-6.33	103.88	δDwax	Wet	Windler et al. (*71*)
off East Java	GeoB10057-3	-8.68	112.87	δDwax	Wet	Ruan et al. (*46*)
Borneo	Gunung Buda	4.00	114.00	$\delta^{18}O_{calcite}$	Dry	Partin et al. (*17*)
Borneo	BJ803-91GGC	2.87	118.39	δDwax	Wet	This study
Sulawesi	Gempa Bumi Cave	-5.00	119.00	$\delta^{18}O_{calcite}$	Wet	Krause et al. (*27*)
Mandar Bay	SO18515	-3.63	119.36	δDwax	Wet	Wicaksono et al. (*72*)
Sulawesi	BJ803-136GGC	-5.93	120.23	δDwax	Wet	This study
Flores	Liang Luar cave	-8.53	120.43	$\delta^{18}O_{calcite}$	Wet	Ayliffe et al. (*43*)
Flores	GeoB10069-3	-9.59	120.92	δDwax	Wet	This study
Sulawesi	Lake Towuti	-2.50	121.50	Ti counts	Dry	Russell et al. (*26*)
Sulawesi	Lake Towuti	-2.73	121.52	δDwax	Wet	Konecky et al. (*73*)
Flores Sea	VM33-80	-7.86	123.00	detrital flux	Wet	Muller et al. (*19*)

[a] HS1 precipitation anomalies (relative to BA) inferred from interpretation in previous literation.
[b] Low temporal resolution. δDwax data from core MD98-2152 only contains one data point during BA. Not included in Cohen's Kappa analysis.

Table S2. List of the sea surface temperature proxy data involved in the proxy synthesis of this study.

Location	Site/Core ID	Lat	Lon	Proxy	Reference
Mozambique channel	GeoB9307-3	-18.57	37.38	Mg/Ca-g.rub	Weldeab et al. (*74*)
off southeast Africa	GIK16160-3	-18.24	37.87	Mg/Ca-g.rub	Wang et al. (*75*)
off East Africa	GeoB12610-2	-4.82	39.42	Mg/Ca-g.rub	Rippert et al. (*76*)
off southeast Africa	GeoB12615-4	-7.14	39.84	Mg/Ca-g.rub	Romahn et al. (*77*)
Arabian Sea	P178-15P	11.96	44.30	Uk'37 & Mg/Ca-g.rub	Tierney et al. (*41*)
off southeast Africa	WIND 28K	-10.15	51.01	Mg/Ca-g.rub	Johnstone et al. (*78*)
Arabian Sea	*TY93929/P	13.70	53.25	Uk'37	Rostek et al. (*79*); Bard et al. (*80*)
Arabian Sea	SO42-74KL	14.32	57.35	Uk'37	Huguet et al. (*81*)
Arabian Sea	*GeoB3007-1	16.17	59.76	Uk'37	Budziak et al. (*82*)
Arabian Sea	AAS9-21	14.51	72.65	Mg/Ca-g.rub	Govil et al. (*83*)
Arabian Sea	SK237-GC04	10.98	75.00	Mg/Ca-g.rub	Saraswat et al. (*84*)
Bay of Bengal	BOB-24	15.57	89.15	Mg/Ca-g.rub	Liu et al. (*85*)
Bay of Bengal	*SO93-126K	19.97	90.03	Uk'37	Kudrass et al. (*86*)
Andaman Sea	ADM-159	9.27	95.61	Mg/Ca-g.rub	Liu et al. (*87*)
off Sumatra	SO189-119KL	3.52	96.32	Mg/Ca-g.rub	Mohtadi et al. (*11*)
off Sumatra	SO189-39KL	-0.78	99.90	Mg/Ca-g.rub	Mohtadi et al. (*11*)
off southern Sumatra	SO139-74KL	-6.54	103.83	Mg/Ca-g.rub	Wang et al. (*88*)
Java Sea	GeoB10043-3	-7.31	105.06	Mg/Ca-g.rub	Setiawan et al. (*89*)
southwest South China Sea	MD01-2390	6.64	113.41	Mg/Ca-g.rub	Steinke et al. (*90*)
Makassar Fan	MD98-2161	-5.21	117.48	Mg/Ca-g.rub	Fan et al. (*91*)
Makassar strait	GIK18519-2	-0.57	118.11	Mg/Ca-g.rub	Schröder et al. (*92*)
Makassar strait	GIK18526-3	-3.61	118.17	Mg/Ca-g.rub	Schröder et al. (*92*)
South of Sunda	MD98-2165	-9.65	118.33	Mg/Ca-g.rub	Levi et al. (*93*)
Celebes Sea	MD98-2178	3.62	118.70	Mg/Ca-g.rub	Fan et al. (*91*)
Celebes Sea	GIK18522-3	1.40	119.08	Mg/Ca-g.rub	Schröder et al. (*92*)
Flores Sea	GIK18540-3	-6.87	119.58	Mg/Ca-g.rub	Schröder et al. (*92*)
Savu Sea	GeoB10069-3	-9.59	120.92	Mg/Ca-g.rub	Gibbons et al. (*94*)
Sulu Sea	MD97-2141	8.47	121.17	Mg/Ca-g.rub	Rosenthal et al. (*95*)
Timor Sea	MD01-2378	-13.08	121.79	Mg/Ca-g.rub	Xu et al. (*96*)
Indonesian Archipelago	TGS-931	-2.41	122.62	Mg/Ca-g.rub	Schröder et al. (*92*)
open ocean near Mindanao	MD06-3067	6.51	126.50	Mg/Ca-g.rub	Bolliet et al. (*97*)
Timor Sea	SO185-18460	-9.09	129.24	Mg/Ca-g.rub	Holbourn et al. (*98*)
Halmahera	MD01-2386	1.01	129.79	Mg/Ca-g.rub	Jian et al. (*99*)

* SST records whose chronology are based on oxygen isotope stratigraphy.

Table S3. List of proxy data used in this study for thermocline depth, reflected by the difference between surface temperature (SST) and thermocline water temperature (TWT).

Region	**Site/Core ID**	**Lat**	**Lon**	**SST**	**TWT**	**Reference**
off East Africa	GeoB12610-2	-4.82	39.42	*G. ruber* Mg/Ca,	*N. dutertrei* Mg/Ca	Rippert et al. (*76*)
off Sumatra	GeoB 10038-4	-5.94	103.3	*G. ruber* Mg/Ca,	*N. dutertrei* Mg/Ca	Mohtadi et al. (*100, 101*)
Timor Sea	MD01-2378	-13.1	121.8	*G. ruber* Mg/Ca,	*P. obliqu*. Mg/Ca	Xu et al. (*96*)
off southern Sumatra	SO139-74KL	-6.54	103.83	*G. ruber* Mg/Ca,	*P. obliqu.* Mg/Ca	Wang et al. (*88*)
East Arabian Sea	BP3-GCR1	15.52	70.01	*G. sacculifer* Mg/Ca	*Gr. tumida* Mg/Ca	Rajasree et al. (*102*)

REFERENCES AND NOTES

1. G. R. McGregor, S. Nieuwolt, *Tropical Climatology: An Introduction to the Climates of the Low Latitudes* (John Wiley & Sons Ltd, ed. 2, 1998).

2. A. C. Clement, R. Seager, M. A. Cane, S. E. Zebiak, An ocean dynamical thermostat. *J. Climate* **9**, 2190–2196 (1996).

3. G. A. Vecchi, B. J. Soden, A. T. Wittenberg, I. M. Held, A. Leetmaa, M. J. Harrison, Weakening of tropical Pacific atmospheric circulation due to anthropogenic forcing. *Nature* **441**, 73–76 (2006).

4. W. Cai, A. Santoso, G. Wang, E. Weller, L. Wu, K. Ashok, Y. Masumoto, T. Yamagata, Increased frequency of extreme Indian Ocean dipole events due to greenhouse warming. *Nature* **510**, 254–258 (2014).

5. X.-T. Zheng, S.-P. Xie, Y. Du, L. Liu, G. Huang, Q. Liu, Indian Ocean dipole response to global warming in the CMIP5 multimodel ensemble. *J. Climate* **26**, 6067–6080 (2013).

6. L. Muntjewerf, M. Petrini, M. Vizcaino, C. Ernani da Silva, R. Sellevold, M. D. W. Scherrenberg, K. Thayer-Calder, S. L. Bradley, J. T. M. Lenaerts, W. H. Lipscomb, M. Lofverstrom, Greenland ice sheet contribution to 21st century sea level rise as simulated by the coupled CESM2.1-CISM2.1. *Geophys. Res. Lett.* **47**, e2019GL086836 (2020).

7. E. Hanna, P. Huybrechts, K. Steffen, J. Cappelen, R. Huff, C. Shuman, T. Irvine-Fynn, S. Wise, M. Griffiths, Increased runoff from melt from the Greenland Ice Sheet: A response to global warming. *J. Climate* **21**, 331–341 (2008).

8. W. Jiang, G. Gastineau, F. Codron, Multicentennial variability driven by salinity exchanges between the atlantic and the arctic ocean in a coupled climate model. *J. Adv. Model. Earth Syst.* **13**, e2020MS002366 (2021).

9. A. Timmermann, Y. Okumura, S.-I. An, A. Clement, B. Dong, E. Guilyardi, A. Hu, J. Jungclaus, M. Renold, T. F. Stocker, The influence of a weakening of the Atlantic meridional overturning circulation on ENSO. *J. Climate* **20**, 4899–4919 (2007).

10. B. Dong, R. T. Sutton, Enhancement of ENSO variability by a weakened atlantic thermohaline circulation in a coupled GCM. *J. Climate* **20**, 4920–4939 (2007).

11. M. Mohtadi, M. Prange, D. W. Oppo, R. De Pol-Holz, U. Merkel, X. Zhang, S. Steinke, A. Luckge, North Atlantic forcing of tropical Indian Ocean climate. *Nature* **509**, 76–80 (2014).

12. J. C. Stager, D. B. Ryves, B. M. Chase, F. S. Pausata, Catastrophic drought in the Afro-Asian monsoon region during Heinrich event 1. *Science* **331**, 1299–1302 (2011).

13. E. Schefuss, H. Kuhlmann, G. Mollenhauer, M. Prange, J. Patzold, Forcing of wet phases in southeast Africa over the past 17,000 years. *Nature* **480**, 509–512 (2011).

14. D. McGee, A. Donohoe, J. Marshall, D. Ferreira, Changes in ITCZ location and cross-equatorial heat transport at the last glacial maximum, Heinrich stadial 1, and the mid-Holocene. *Earth Planet. Sci. Lett.* **390**, 69–79 (2014).

15. G. Deplazes, A. Lückge, L. C. Peterson, A. Timmermann, Y. Hamann, K. A. Hughen, U. Röhl, C. Laj, M. A. Cane, D. M. Sigman, G. H. Haug, Links between tropical rainfall and North Atlantic climate during the last glacial period. *Nat. Geosci.* **6**, 213–217 (2013).

16. L. C. Peterson, G. H. Haug, K. A. Hughen, U. Röhl, Rapid changes in the hydrologic cycle of the tropical atlantic during the last glacial. *Science* **290**, 1947–1951 (2000).

17. J. W. Partin, K. M. Cobb, J. F. Adkins, B. Clark, D. P. Fernandez, Millennial-scale trends in west Pacific warm pool hydrology since the last glacial maximum. *Nature* **449**, 452–453 (2007).

18. P. A. Baker, S. C. Fritz, Nature and causes of Quaternary climate variation of tropical South America. *Quat. Sci. Rev.* **124**, 31–47 (2015).

19. J. Muller, J. F. McManus, D. W. Oppo, R. Francois, Strengthening of the Northeast Monsoon over the Flores Sea, Indonesia, at the time of Heinrich event 1. *Geology* **40**, 635–638 (2012).

20. X. Wang, A. S. Auler, R. L. Edwards, H. Cheng, P. S. Cristalli, P. L. Smart, D. A. Richards, C.-C. Shen, Wet periods in northeastern Brazil over the past 210 kyr linked to distant climate anomalies. *Nature* **432**, 740–743 (2004).

21. P. A. Baker, S. C. Fritz, S. J. Burns, E. Ekdahl, C. A. Rigsby, The nature and origin of decadal to millennial scale climate variability in the southern tropics of South America: The Holocene record of Lago Umayo, Peru, in *Past Climate Variability in South America and Surrounding Regions* (Springer, 2009), pp. 301–322.

22. E. M. Niedermeyer, A. L. Sessions, S. J. Feakins, M. Mohtadi, Hydroclimate of the western Indo-Pacific warm pool during the past 24,000 years. *Proc. Natl. Acad. Sci. U.S.A.* **111**, 9402–9406 (2014).

23. C. He, Z. Liu, B. L. Otto-Bliesner, E. C. Brady, C. Zhu, R. Tomas, P. U. Clark, J. Zhu, A. Jahn, S. Gu, J. Zhang, J. Nusbaumer, D. Noone, H. Cheng, Y. Wang, M. Yan, Y. Bao, Hydroclimate footprint of pan-Asian monsoon water isotope during the last deglaciation. *Sci. Adv.* **7**, eabe2611 (2021).

24. X. Du, J. M. Russell, Z. Liu, B. L. Otto-Bliesner, Y. Gao, C. Zhu, D. W. Oppo, M. Mohtadi, Y. Yan, V. V. Galy, C. He, Deglacial trends in Indo-Pacific warm pool hydroclimate in an isotope-enabled Earth system model and implications for isotope-based paleoclimate reconstructions. *Quat. Sci. Rev.* **270**, 107188 (2021).

25. C. He, Z. Liu, L. Otto-Bliesner Bette, C. Brady Esther, C. Zhu, R. Tomas, C. Buizert, P. Severinghaus Jeffrey, Abrupt Heinrich Stadial 1 cooling missing in Greenland oxygen isotopes. *Sci. Adv.* **7**, eabh1007.

26. J. M. Russell, H. Vogel, B. L. Konecky, S. Bijaksana, Y. S. Huang, M. Melles, N. Wattrus, K. Costa, J. W. King, Glacial forcing of central Indonesian hydroclimate since 60,000 y B.P. *Proc. Natl. Acad. Sci. U.S.A.* **111**, 5100–5105 (2014).

27. C. E. Krause, M. K. Gagan, G. B. Dunbar, W. S. Hantoro, J. C. Hellstrom, H. Cheng, R. L. Edwards, B. W. Suwargadi, N. J. Abram, H. Rifai, Spatio-temporal evolution of Australasian monsoon hydroclimate over the last 40,000 years. *Earth Planet. Sci. Lett.* **513**, 103–112 (2019).

28. D. Mcgee, E. Moreno-Chamarro, B. Green, J. Marshall, E. Galbraith, L. Bradtmiller, Hemispherically asymmetric trade wind changes as signatures of past ITCZ shifts. *Quat. Sci. Rev.* **180**, 214–228 (2018).

29. J. C. H. Chiang, A. R. Friedman, Extratropical cooling, interhemispheric thermal gradients, and tropical climate change. *Annu. Rev. Earth Planet. Sci.* **40**, 383–412 (2012).

30. I. Cvijanovic, J. C. H. Chiang, Global energy budget changes to high latitude North Atlantic cooling and the tropical ITCZ response. *Climate Dynam.* **40**, 1435–1452 (2013).

31. J. Bjerknes, Atmospheric teleconnections from the equatorial PACIFIC1. *Mon. Weather Rev.* **97**, 163–172 (1969).

32. K. Thirumalai, P. N. DiNezio, J. E. Tierney, M. Puy, M. Mohtadi, An El Niño mode in the Glacial Indian Ocean? *Paleoceanogr. Paleoclimatol.* **34**, 1316–1327 (2019).

33. P. N. DiNezio, M. Puy, K. Thirumalai, F.-F. Jin, J. E. Tierney, Emergence of an equatorial mode of climate variability in the Indian Ocean. *Sci. Adv.* **6**, eaay7684 (2020).

34. P. N. DiNezio, J. E. Tierney, The effect of sea level on glacial Indo-Pacific climate. *Nat. Geosci.* **6**, 485–491 (2013).

35. P. N. DiNezio, J. E. Tierney, B. L. Otto-Bliesner, A. Timmermann, T. Bhattacharya, N. Rosenbloom, E. Brady, Glacial changes in tropical climate amplified by the Indian Ocean. *Sci. Adv.* **4**, eaat9658 (2018).

36. P. N. Di Nezio, A. Timmermann, J. E. Tierney, F.-F. Jin, B. Otto-Bliesner, N. Rosenbloom, B. Mapes, R. Neale, R. F. Ivanovic, A. Montenegro, The climate response of the Indo-Pacific warm pool to glacial sea level. *Paleoceanography* **31**, 866–894 (2016).

37. D. Verschuren, J. S. S. Damste, J. Moernaut, I. Kristen, M. Blaauw, M. Fagot, G. H. Haug; CHALLACEA project members, Half-precessional dynamics of monsoon rainfall near the East African equator. *Nature* **462**, 637–641 (2009).

38. I. S. Castañeda, J. P. Werne, T. C. Johnson, Wet and arid phases in the southeast African tropics since the last glacial maximum. *Geology* **35**, 823–826 (2007).

39. B. L. Konecky, J. M. Russell, T. C. Johnson, E. T. Brown, M. A. Berke, J. P. Werne, Y. Huang, Atmospheric circulation patterns during late Pleistocene climate changes at Lake Malawi, Africa. *Earth Planet. Sci. Lett.* **312**, 318–326 (2011).

40. J. E. Tierney, J. M. Russell, Y. S. Huang, J. S. S. Damste, E. C. Hopmans, A. S. Cohen, Northern hemisphere controls on tropical southeast African climate during the past 60,000 years. *Science* **322**, 252–255 (2008).

41. J. E. Tierney, F. S. R. Pausata, P. DeMenocal, Deglacial Indian monsoon failure and North Atlantic stadials linked by Indian Ocean surface cooling. *Nat. Geosci.* **9**, 46–50 (2016).

42. C. Johnson Thomas, A. Scholz Christopher, R. Talbot Michael, K. Kelts, R. D. Ricketts, G. Ngobi, K. Beuning, I. Ssemmanda, J. W. McGill, Late pleistocene desiccation of lake victoria and rapid evolution of cichlid fishes. *Science* **273**, 1091–1093 (1996).

43. L. K. Ayliffe, M. K. Gagan, J.-x. Zhao, R. N. Drysdale, J. C. Hellstrom, W. S. Hantoro, M. L. Griffiths, H. Scott-Gagan, E. S. Pierre, J. A. Cowley, B. W. Suwargadi, Rapid interhemispheric climate links via the Australasian monsoon during the last deglaciation. *Nat. Commun.* **4**, 2908 (2013).

44. S. van der Kaars, F. Bassinot, P. De Deckker, F. Guichard, Changes in monsoon and ocean circulation and the vegetation cover of southwest Sumatra through the last 83,000years: The record from marine core BAR94-42. *Palaeogeogr. Palaeoclimatol. Palaeoecol.* **296**, 52–78 (2010).

45. M. Mohtadi, S. Steinke, A. Lückge, J. Groeneveld, E. C. Hathorne, Glacial to Holocene surface hydrography of the tropical eastern Indian Ocean. *Earth Planet. Sci. Lett.* **292**, 89–97 (2010).

46. Y. Ruan, M. Mohtadi, S. van der Kaars, L. M. Dupont, D. Hebbeln, E. Schefuß, Differential hydro-climatic evolution of East Javanese ecosystems over the past 22,000 years. *Quat. Sci. Rev.* **218**, 49–60 (2019).

47. D. Yuan, H. Cheng, R. L. Edwards, C. A. Dykoski, M. J. Kelly, M. Zhang, J. Qing, Y. Lin, Y. Wang, J. Wu, Timing, duration, and transitions of the last interglacial Asian monsoon. *Science* **304**, 575–578 (2004).

48. Y. J. Wang, H. Cheng, R. L. Edwards, Z. S. An, J. Y. Wu, C. C. Shen, J. A. Dorale, A high-resolution absolute-dated late pleistocene monsoon record from Hulu Cave, China. *Science* **294**, 2345–2348 (2001).

49. F. S. Pausata, D. S. Battisti, K. H. Nisancioglu, C. M. Bitz, Chinese stalagmite $\delta^{18}O$ controlled by changes in the Indian monsoon during a simulated Heinrich event. *Nat. Geosci.* **4**, 474–480 (2011).

50. S. Lewis, A. LeGrande, M. Kelley, G. Schmidt, Water vapour source impacts on oxygen isotope variability in tropical precipitation during Heinrich events. *Clim. Past* **6**, 325–343 (2010).

51. E. Brady, S. Stevenson, D. Bailey, Z. Liu, D. Noone, J. Nusbaumer, B. L. Otto-Bliesner, C. Tabor, R. Tomas, T. Wong, J. Zhang, J. Zhu, The connected isotopic water cycle in the community earth system model version 1. *J. Adv. Model. Earth Syst.* **11**, 2547–2566 (2019).

52. W. R. Peltier, D. F. Argus, R. Drummond, Space geodesy constrains ice age terminal deglaciation: The global ICE-6G_C (VM5a) model. *J. Geophys. Res. Solid Earth* **120**, 450–487 (2015).

53. D. Lüthi, M. Le Floch, B. Bereiter, T. Blunier, J.-M. Barnola, U. Siegenthaler, D. Raynaud, J. Jouzel, H. Fischer, K. Kawamura, T. F. Stocker, High-resolution carbon dioxide concentration record 650,000–800,000 years before present. *Nature* **453**, 379–382 (2008).

54. J. R. Petit, J. Jouzel, D. Raynaud, N. I. Barkov, J. M. Barnola, I. Basile, M. Bender, J. Chappellaz, M. Davis, G. Delaygue, M. Delmotte, V. M. Kotlyakov, M. Legrand, V. Y. Lipenkov, C. Lorius, L. PÉpin, C. Ritz, E. Saltzman, M. Stievenard, Climate and atmospheric history of the past 420,000 years from the Vostok ice core, Antarctica. *Nature* **399**, 429–436 (1999).

55. A. Schilt, M. Baumgartner, T. Blunier, J. Schwander, R. Spahni, H. Fischer, T. F. Stocker, Glacial–Interglacial and millennial-scale variations in the atmospheric nitrous oxide concentration during the last 800,000 years. *Quat. Sci. Rev.* **29**, 182–192 (2010).

56. Z. Liu, B. L. Otto-Bliesner, F. He, E. C. Brady, R. Tomas, P. U. Clark, A. E. Carlson, J. Lynch-Stieglitz, W. Curry, E. Brook, D. Erickson, R. Jacob, J. Kutzbach, J. Cheng, Transient simulation of last deglaciation with a new mechanism for bolling-allerod warming. *Science* **325**, 310–314 (2009).

57. S. Stevenson, B. Otto-Bliesner, E. Brady, J. Nusbaumer, C. Tabor, R. Tomas, D. Noone, Z. Liu, Volcanic eruption signatures in the isotope-enabled last millennium ensemble. *Paleoceanogr. Paleoclimatol.* **34**, 1534–1552 (2019).

58. R. F. Adler, G. J. Huffman, A. Chang, R. Ferraro, P.-P. Xie, J. Janowiak, B. Rudolf, U. Schneider, S. Curtis, D. Bolvin, A. Gruber, J. Susskind, P. Arkin, E. Nelkin, The version-2 global precipitation climatology project (GPCP) monthly precipitation analysis (1979–present). *J. Hydrometeorol.* **4**, 1147–1167 (2003).

59. T. J. Heaton, P. Köhler, M. Butzin, E. Bard, R. W. Reimer, W. E. N. Austin, C. Bronk Ramsey, P. M. Grootes, K. A. Hughen, B. Kromer, P. J. Reimer, J. Adkins, A. Burke, M. S. Cook, J. Olsen, L. C. Skinner, Marine20—The marine radiocarbon age calibration curve (0–55,000 cal BP). *Radiocarbon* **62**, 779–820 (2020).

60. P. J. Reimer, W. E. N. Austin, E. Bard, A. Bayliss, P. G. Blackwell, C. B. Ramsey, M. Butzin, H. Cheng, R. L. Edwards, M. Friedrich, P. M. Grootes, T. P. Guilderson, I. Hajdas, T. J. Heaton, A. G. Hogg, K. A. Hughen, B. Kromer, S. W. Manning, R. Muscheler, J. G. Palmer, C. Pearson, J. van der Plicht, R. W. Reimer, D. A. Richards, E. M. Scott, J. R. Southon, C. S. M. Turney, L. Wacker, F. Adolphi, U. Büntgen, M. Capano, S. M. Fahrni, A. Fogtmann-Schulz, R. Friedrich, P. Köhler, S. Kudsk, F. Miyake, J. Olsen, F. Reinig, M. Sakamoto, A. Sookdeo, S. Talamo, The IntCal20 Northern Hemisphere Radiocarbon Age Calibration Curve (0–55 cal kBP). *Radiocarbon* **62**, 725–757 (2020).

61. M. Blaauw, J. A. Christen, Flexible paleoclimate age-depth models using an autoregressive gamma process. *Bayesian Anal.* **6**, 457–474 (2011).

62. A. Vincens, G. Buchet, D. Williamson, M. Taieb, A 23,000 yr pollen record from Lake Rukwa (8°S, SW Tanzania): New data on vegetation dynamics and climate in Central Eastern Africa. *Rev. Palaeobot. Palynol.* **137**, 147–162 (2005).

63. J. C. Stager, P. A. Mayewski, L. D. Meeker, Cooling cycles, Heinrich event 1, and the desiccation of Lake Victoria. *Palaeogeogr. Palaeoclimatol. Palaeoecol.* **183**, 169–178 (2002).

64. E. Parzen, On estimation of a probability density function and mode. *Ann. Math. Stat.* **33**, 1065–1076 (1962).

65. P. Barker, D. Williamson, F. Gasse, E. Gibert, Climatic and volcanic forcing revealed in a 50,000-year diatom record from Lake Massoko, Tanzania. *Quatern. Res.* **60**, 368–376 (2003).

66. K. Costa, J. Russell, B. Konecky, H. Lamb, Isotopic reconstruction of the African Humid Period and Congo Air Boundary migration at Lake Tana, Ethiopia. *Quat. Sci. Rev.* **83**, 58–67 (2014).

67. S. Garelick, J. M. Russell, S. Dee, D. Verschuren, D. O. Olago, Atmospheric controls on precipitation isotopes and hydroclimate in high-elevation regions in Eastern Africa since the Last Glacial Maximum. *Earth Planet. Sci. Lett.* **567**, 116984 (2021).

68. J. E. Tierney, J. M. Russell, J. S. Sinninghe Damsté, Y. Huang, D. Verschuren, Late quaternary behavior of the East African monsoon and the importance of the Congo Air Boundary. *Quat. Sci. Rev.* **30**, 798–807 (2011).

69. J. E. Tierney, P. B. DeMenocal, Abrupt shifts in Horn of Africa hydroclimate since the last glacial maximum. *Science* **342**, 843–846 (2013).

70. J. D. Shakun, S. J. Burns, D. Fleitmann, J. Kramers, A. Matter, A. Al-Subary, A high-resolution, absolute-dated deglacial speleothem record of Indian Ocean climate from Socotra Island, Yemen. *Earth Planet. Sci. Lett.* **259**, 442–456 (2007).

71. G. Windler, J. E. Tierney, J. Zhu, C. J. Poulsen, Unraveling glacial hydroclimate in the Indo-Pacific Warm Pool: Perspectives from water isotopes. *Paleoceanogr. Paleoclimatol.* **35**, e2020PA003985 (2020).

72. S. A. Wicaksono, J. M. Russell, A. Holbourn, W. Kuhnt, Hydrological and vegetation shifts in the Wallacean region of central Indonesia since the Last Glacial Maximum. *Quat. Sci. Rev.* **157**, 152–163 (2017).

73. B. Konecky, J. Russell, S. Bijaksana, Glacial aridity in central Indonesia coeval with intensified monsoon circulation. *Earth Planet. Sci. Lett.* **437**, 15–24 (2016).

74. S. Weldeab, D. W. Lea, H. Oberhänsli, R. R. Schneider, Links between southwestern tropical Indian Ocean SST and precipitation over southeastern Africa over the last 17kyr. *Palaeogeogr. Palaeoclimatol. Palaeoecol.* **410**, 200–212 (2014).

75. Y. V. Wang, G. Leduc, M. Regenberg, N. Andersen, T. Larsen, T. Blanz, R. R. Schneider, Northern and southern hemisphere controls on seasonal sea surface temperatures in the Indian Ocean during the last deglaciation. *Paleoceanography* **28**, 619–632 (2013).

76. N. Rippert, K.-H. Baumann, J. PÄTzold, Thermocline fluctuations in the western tropical Indian Ocean during the past 35 ka. *J. Quat. Sci.* **30**, 201–210 (2015).

77. S. Romahn, A. Mackensen, J. Groeneveld, J. Pätzold, Deglacial intermediate water reorganization: New evidence from the Indian Ocean. *Climate Past* **10**, 293–303 (2014).

78. H. J. H. Johnstone, T. Kiefer, H. Elderfield, M. Schulz, Calcite saturation, foraminiferal test mass, and Mg/Ca-based temperatures dissolution corrected using XDX—A 150 ka record from the western Indian Ocean. *Geochemistry Geophys. Geosystems* **15**, 781–797 (2014).

79. F. Rostek, E. Bard, L. Beaufort, C. Sonzogni, G. Ganssen, Sea surface temperature and productivity records for the past 240 kyr in the Arabian Sea. *Deep Sea Res. Part II Top. Stud. Oceanogr.* **44**, 1461–1480 (1997).

80. E. Bard, F. Rostek, C. Sonzogni, Interhemispheric synchrony of the last deglaciation inferred from alkenone palaeothermometry. *Nature* **385**, 707–710 (1997).

81. C. Huguet, J. H. Kim, J. S. Sinninghe Damsté, S. Schouten, Reconstruction of sea surface temperature variations in the Arabian Sea over the last 23 kyr using organic proxies (TEX_{86} and $U37^{K'}$). *Paleoceanography* **21**, PA3003 (2006).

82. D. Budziak, Late Quaternary monsoonal climate and related variations in paleoproductivity and alkenone-derived sea-surface temperatures in the western Arabian Sea. *Berichte, Fachbereich Geowissenschaften, Universität Bremen* (2001).

83. P. Govil, P. D. Naidu, Evaporation-precipitation changes in the eastern Arabian Sea for the last 68 ka: Implications on monsoon variability. *Paleoceanography* **25**, PA1210 (2010).

84. R. Saraswat, D. W. Lea, R. Nigam, A. Mackensen, D. K. Naik, Deglaciation in the tropical Indian Ocean driven by interplay between the regional monsoon and global teleconnections. *Earth Planet. Sci. Lett.* **375**, 166–175 (2013).

85. S. Liu, W. Ye, M.-T. Chen, H.-J. Pan, P. Cao, H. Zhang, S. Khokiattiwong, N. Kornkanitnan, X. Shi, Millennial-scale variability of Indian summer monsoon during the last 42 kyr: Evidence based on foraminiferal Mg/Ca and oxygen isotope records from the central Bay of Bengal. *Palaeogeogr. Palaeoclimatol. Palaeoecol.* **562**, 110112 (2021), 110112.

86. H. R. Kudrass, A. Hofmann, H. Doose, K. Emeis, H. Erlenkeuser, Modulation and amplification of climatic changes in the Northern Hemisphere by the Indian summer monsoon during the past 80 k.y. *Geology* **29**, 63–66 (2001).

87. S. Liu, W. Ye, P. Cao, H. Zhang, M.-T. Chen, X. Li, J. Li, H.-J. Pan, S. Khokiattiwong, N. Kornkanitnan, X. Shi, Paleoclimatic responses in the tropical Indian Ocean to regional monsoon and global climate change over the last 42 kyr. *Mar. Geol.* **438**, 106542 (2021).

88. X. Wang, Z. Jian, A. Lückge, Y. Wang, H. Dang, M. Mohtadi, Precession-paced thermocline water temperature changes in response to upwelling conditions off southern Sumatra over the past 300,000 years. *Quat. Sci. Rev.* **192**, 123–134 (2018).

89. R. Y. Setiawan, M. Mohtadi, J. Southon, J. Groeneveld, S. Steinke, D. Hebbeln, The consequences of opening the Sunda Strait on the hydrography of the eastern tropical Indian Ocean. *Paleoceanography* **30**, 1358–1372 (2015).

90. S. Steinke, H.-Y. Chiu, P.-S. Yu, C.-C. Shen, H. Erlenkeuser, L. Löwemark, M.-T. Chen, On the influence of sea level and monsoon climate on the southern South China Sea freshwater budget over the last 22,000 years. *Quat. Sci. Rev.* **25**, 1475–1488 (2006).

91. W. Fan, Z. Jian, Z. Chu, H. Dang, Y. Wang, F. Bassinot, X. Han, Y. Bian, Variability of the Indonesian Throughflow in the Makassar Strait over the last 30 ka. *Sci. Rep.* **8**, 5678 (2018).

92. J. F. Schröder, W. Kuhnt, A. Holbourn, S. Beil, P. Zhang, M. Hendrizan, J. Xu, Deglacial warming and hydroclimate variability in the central Indonesian archipelago. *Paleoceanogr. Paleoclimatol.* **33**, 974–993 (2018).

93. C. Levi, L. Labeyrie, F. Bassinot, F. Guichard, E. Cortijo, C. Waelbroeck, N. Caillon, J. Duprat, T. de Garidel-Thoron, H. Elderfield, Low-latitude hydrological cycle and rapid climate changes during the last deglaciation. *Geochem. Geophys. Geosytems* **8**, Q05N12 (2007).

94. F. T. Gibbons, D. W. Oppo, M. Mohtadi, Y. Rosenthal, J. Cheng, Z. Liu, B. K. Linsley, Deglacial δ18O and hydrologic variability in the tropical Pacific and Indian Oceans. *Earth Planet. Sci. Lett.* **387**, 240–251 (2014).

95. Y. Rosenthal, D. W. Oppo, B. K. Linsley, The amplitude and phasing of climate change during the last deglaciation in the Sulu Sea, western equatorial Pacific. *Geophys. Res. Lett.* **30**, 1428 (2003).

96. J. Xu, A. Holbourn, W. Kuhnt, Z. Jian, H. Kawamura, Changes in the thermocline structure of the Indonesian outflow during Terminations I and II. *Earth Planet. Sci. Lett.* **273**, 152–162 (2008).

97. T. Bolliet, A. Holbourn, W. Kuhnt, C. Laj, C. Kissel, L. Beaufort, M. Kienast, N. Andersen, D. Garbe-Schönberg, Mindanao Dome variability over the last 160 kyr: Episodic glacial cooling of the West Pacific warm pool. *Paleoceanography* **26**, PA1208 (2011).

98. A. Holbourn, W. Kuhnt, J. Xu, Indonesian Throughflow variability during the last 140 ka: The Timor Sea outflow. *Geol. Soc. Spec. Publ.* **355**, 283–303 (2011).

99. Z. Jian, Y. Wang, H. Dang, D. W. Lea, Z. Liu, H. Jin, Y. Yin, Half-precessional cycle of thermocline temperature in the western equatorial Pacific and its bihemispheric dynamics. *Proc. Natl. Acad. Sci. U.S.A.* **117**, 7044–7051 (2020).

100. M. Mohtadi, A. Lückge, S. Steinke, J. Groeneveld, D. Hebbeln, N. Westphal, Late Pleistocene surface and thermocline conditions of the eastern tropical Indian Ocean. *Quat. Sci. Rev.* **29**, 887–896 (2010).

101. M. Mohtadi, M. Prange, E. Schefuss, T. C. Jennerjahn, Late Holocene slowdown of the Indian Ocean Walker circulation. *Nat. Commun.* **8**, 1015 (2017).

102. A. Rajasree, V. R. Punyu, V. K. Banakar, Last 35,000-year water column temperature and productivity variation in the Eastern Arabian Sea: Monsoon and global climate connection. *Geo-Marine Lett.* **39**, 239–248 (2019).